The novel Cer-like protein Caronte mediates the establishment of embryonic left–right asymmetry

Concepción Rodríguez Esteban*†, Javier Capdevila*†, Aris N. Economides‡, Jaime Pascual§, Ángel Ortiz§ & Juan Carlos Izpisúa Belmonte*

* *The Salk Institute for Biological Studies, Gene Expression Laboratory, 10010 North Torrey Pines Road, La Jolla, California 92037, USA*
‡ *Regeneron Pharmaceuticals, Inc., 777 Old Saw Mill River Road, Tarrytown, New York 10591, USA*
§ *Department of Molecular Biology, The Scripps Research Institute, 10550 North Torrey Pines Road, La Jolla, California 92037, USA*
† *These authors contributed equally to this work*

In the chick embryo, left–right asymmetric patterns of gene expression in the lateral plate mesoderm are initiated by signals located in and around Hensen's node. Here we show that Caronte (Car), a secreted protein encoded by a member of the *Cerberus/Dan* gene family, mediates the *Sonic hedgehog* (*Shh*)-dependent induction of left-specific genes in the lateral plate mesoderm. *Car* is induced by Shh and repressed by fibroblast growth factor-8 (FGF-8). Car activates the expression of *Nodal* by antagonizing a repressive activity of bone morphogenic proteins (BMPs). Our results define a complex network of antagonistic molecular interactions between Activin, FGF-8, Lefty-1, Nodal, BMPs and Car that cooperate to control left–right asymmetry in the chick embryo.

Many of the cellular and molecular events involved in the establishment of left–right asymmetry in vertebrates are now understood. Following the discovery of the first genes asymmetrically expressed in the chick embryo[1], a model of left–right determination involving a complex cascade of genetic interactions has emerged[2–4]. The model explains how inductive signals initiated in or near the organizer region of the gastrulating embryo control the establishment of asymmetric patterns of gene expression throughout the lateral plate mesoderm (LPM). These asymmetric patterns are interpreted during development to give rise to left–right asymmetries of internal organs and other embryonic structures.

Nodal is crucial in establishing initial left–right cues in the vertebrate embryo. The expression of *Nodal* in the left LPM is strictly correlated with the development of normal organ *situs* in all vertebrates examined so far[5–7]. Furthermore, misexpression of *Nodal* alters left–right development in chick and *Xenopus* embryos[1,8–10]. Although *Shh* expression in the node is necessary and sufficient to induce *Nodal* in the left LPM[10], its exact mechanism is largely unknown. As the action of Shh seems to be restricted to cells immediately adjacent to the node, it is difficult to foresee how it could directly activate *Nodal* expression in the left LPM, far away from the node. Tissue explant experiments[10] and the study of laterality defects in conjoined twins[11] led to the proposal that *Shh* induces *Nodal* in the LPM through an unknown ('X') secondary signal that is active in the paraxial tissue immediately adjacent to the midline[10].

Here we describe the isolation and characterization of a long-range signal, Caronte (Car), that fulfils the criteria to be such a secondary signal. *Car*, which is expressed in the left paraxial chick mesoderm, is necessary and sufficient to transmit the Shh signal from the node to the left LPM, leading to *Nodal* activation and subsequent establishment of left–right-specific gene expression. Moreover, we provide evidence (by combining *in vivo* misexpression experiments, *in vitro* binding studies, sequence analysis and modelling tools) that Car might activate *Nodal* in the left LPM by relieving a repressive effect of BMPs on *Nodal* transcription, revealing that BMP antagonism is involved in mediating the transfer of left–right positional information from the organizer region to the LPM.

If the initial establishment of asymmetric gene expression in the LPM is essential for proper development, it is equally important to ensure that asymmetry is maintained throughout embryogenesis. An important factor in this regard is Lefty-1, another transforming growth factor-β (TGF-β) family member, that has been proposed to act as a molecular midline barrier that would confine and prevent the 'X' factor from diffusing from the left to the right side of the embryo[12,13]. Here we show that an excess of Lefty-1 in the left side of the embryo blocks activation of *Nodal* by *Car*. The opposite experiment, ectopic application of Lefty-1 on the right side, downregulates the expression of the right-sided genes *FGF-8* (ref. 14) (which, in turn, can downregulate *Car* expression) and *chicken Snail related*[15] (*cSnr*), and upregulates left-sided genes (*Car*, *Nodal* and *Pitx2*). We also show that Car can induce expression of *Lefty-1*. Together, these results uncover a network of molecular interactions that involves a delicate balance of TGF-β activity (including Activin, Lefty-1, BMPs and Nodal) and two other secreted factors, FGF-8 and Car, which modulate and restrict the activity of these TGF-βs, allowing proper establishment of the left–right axis.

The molecular interactions described above establish broad domains of side-specific gene expression in the embryo that are translated into specific left–right asymmetric development of organs. *Pitx2* (refs 16, 17; see also ref. 2 and references therein) and *cSnR*[15] are targets of the left–right signalling cascade initiated at gastrulation. We have identified *cNKX3.2*, a new homeobox gene that, like *Pitx2*, may interpret and execute the developmental program dictated by the upstream signalling cascade, so that proper left–right organ asymmetry ensues.

Novel genes involved in left–right development

A novel *Cer*-like gene, the chick *NKX3.2* gene and the chick *Lefty-1* gene were isolated in a screening designed to identify genes specifically expressed in the left LPM (see Methods). We named the novel *Cer*-like gene *Caronte* (*Car*), after the boatman who ferried the souls of the dead across the River Styx in Greek mythology. It encodes a predicted protein of 273 amino acids and contains a hydrophobic signal sequence at the amino terminus and a carboxy-terminal cysteine-knot (CTCK) motif from amino-acids 167 to 244. Sequence comparisons, along with the expression pattern and

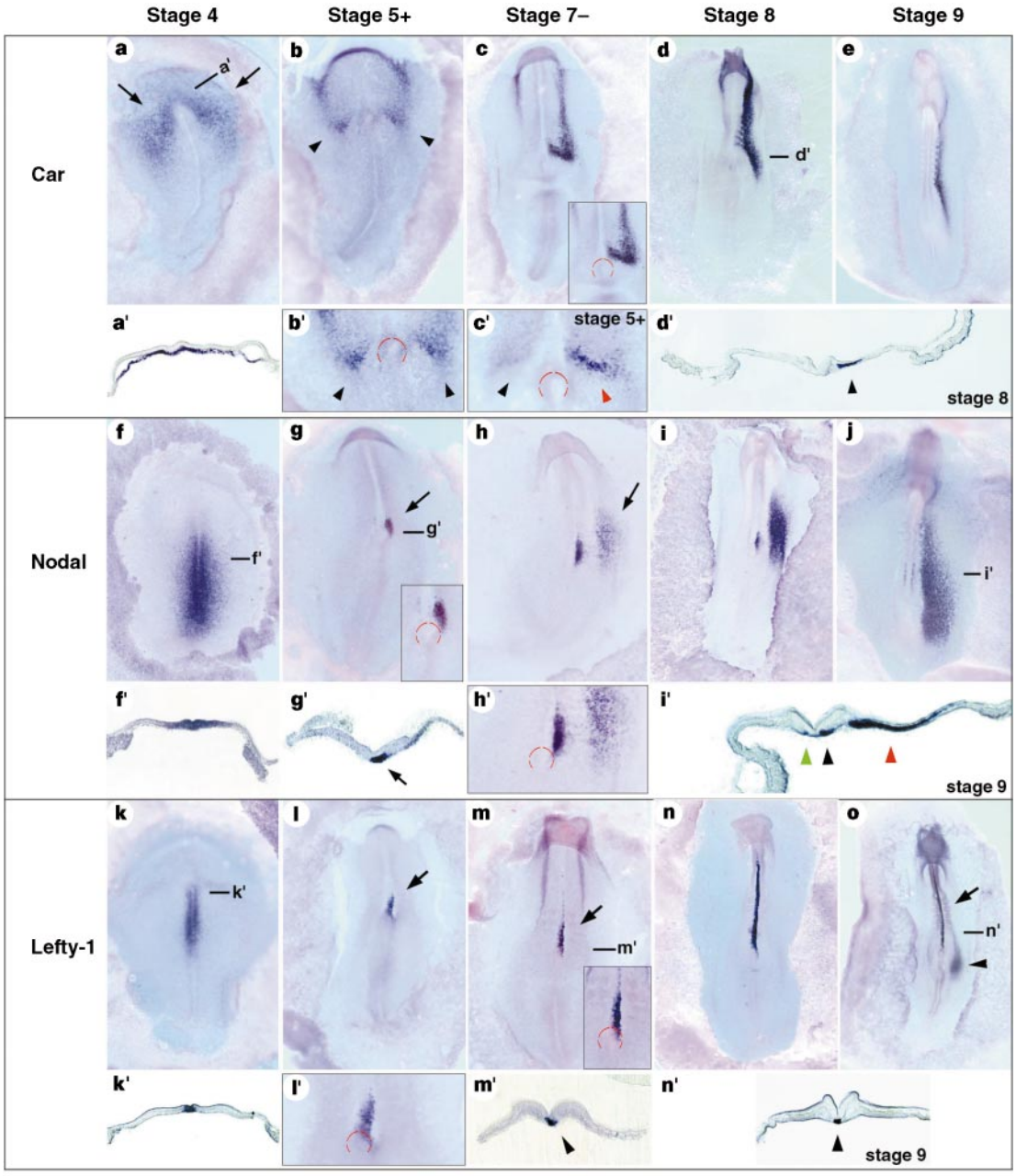

Figure 1 Expression of *Car*, *Nodal* and *Lefty-1* during chick gastrulation. Embryos in all panels are viewed from the ventral side; the left side of the embryo is to the right in all panels unless otherwise indicated. **a**, At stage 4, *Car* is expressed bilaterally in the perinodal region (arrows). **a′**, Cross-section showing expression of *Car* restricted to the mesodermal layer. **b**, Stage 5+ embryo showing symmetrical distribution of *Car* transcripts, with two patches of strong expression flanking Hensen's node (arrowheads). **b′**, Higher magnification of **b**. The node is delineated in red in this and subsequent panels. **c′**, At stages 5+ to 6, the right perinodal expression of *Car* is downregulated. Some embryos at stage 5+ already show strong *Car* expression on the left side (red arrowhead) and almost no expression on the right (black arrowhead). The staining on the left side is adjacent to cells expressing *Nodal* (**g**, inset) and *Lefty-1* (**l**, **l′**). **c**, At stage 7–, *Car* is stronger on the left head mesoderm than on the right (inset, left-specific perinodal expression). **d**, At stage 8, a second domain of *Car* expression appears in the left LPM, extending anteriorly and caudally. **e**, At stage 9, *Car* transcripts start to fade. **d′**, Cross-section of the embryo in **d** showing expression of *Car* in the left LPM (arrowhead). **f**, *Nodal* transcripts are symmetrically expressed in the posterior two-thirds of the primitive streak at stage 4. **f′**, Cross-section of the embryo in **f** showing *Nodal* staining in ectoderm and mesendoderm. **g**, Stage 5+ embryo showing asymmetric expression of *Nodal* in cells adjacent to the left side of Hensen's node (arrow). Inset, higher magnification of the node. **g′**, Cross-section of the embryo in **g** showing staining of *Nodal* on the left mesodermal layer (arrow). **h**, Stage 7– embryo showing a second domain of *Nodal* expression in the left LPM (arrow). **h′**, Perinodal expression of *Nodal*, still restricted to the left. **i**, Stage 8 embryo showing Nodal expression similar to that in **h**. **j**, At stage 9, *Nodal* expands throughout the left LPM (red arrowhead in **i′**) and is expressed not only on the left side of the midline (black arrowhead), but also on the right side (green arrowhead). **k**, At stage 4, *Lefty-1* transcripts are restricted to the anterior half of the primitive streak. **k′**, Cross-section of the embryo in **k** with expression in ectoderm and mesendoderm. **l**, At stage 5+, *Lefty-1* transcripts are expressed asymmetrically in the left side of the node (arrow; see higher magnification in **l′**). **m**, Stage 7– embryo showing *Lefty-1* expression on the left side of the node and the left side of the prechordal mesoderm (arrow; see inset for detail). **m′**, Cross-section of the embryo in **m** depicting expression of *Lefty-1* on the left side of the midline (arrowhead). **n**, Stage 8 embryo. *Lefty-1* midline expression has expanded towards the anterior side of the embryo. **o**, At stage 9, *Lefty-1* expression is symmetrically distributed throughout the notochord (arrow; see also arrowhead in cross-section in **n′**). A patch of *Lefty-1* expression is now detected on the posterior left LPM (arrowhead in **o**).

functional assays described below, indicate that *Car* is a member of the *Cer/Dan* gene family. Other members of this family include *Xenopus Cerberus*[18], *gremlin* (identified in several organisms)[19], and the mouse genes *Dan*[20,21], *Cer1* (refs 22–24), *Drm*[19,25] and *Dante*[26]. Members of the Cer/Dan family of secreted factors are important for patterning the embryo by antagonizing the activities of BMPs and other secreted proteins. The *Car* gene was independently isolated by two other groups[27,28].

A second isolated gene fragment translates into a 141-amino-acid sequence that shows homology to Lefty proteins. The full-length gene was obtained by screening a genomic chick library. The predicted amino-acid sequence shows 60% identity to the zebrafish *Antivin*[29], 38% identity to mouse *Lefty-1* (refs 30, 31) and 34% identity to mouse *Lefty-2* (ref. 30). Thus, this gene appears to be the chick orthologue of zebrafish *Antivin*. However, based on sequence comparison we cannot tell whether the chick gene is the orthologue of mouse *Lefty-1* or *Lefty-2*. As its pattern of expression closely resembles that of mouse *Lefty-1*, and as Antivin and Lefty-1 are functionally equivalent[29], we will call the isolated gene *Lefty-1* hereafter until the putative second *Lefty* is isolated in the chick. Similar nomenclature has been adopted by S. Noji *et al.* (personal communication).

The chick *NKX3.2* gene encodes a 276-amino-acid protein that contains a homeobox from residues 151 to 207 which shows 98% identity with the homeoboxes of the Human *bagpipe*, mouse *NKX3.2*, *Xenopus bagpipe* and *Pleurodeles waltl Nkx3.2* genes. The high degree of conservation of these proteins extends to their C termini. *cNKX3.2* was also independently isolated by another group[32].

Car induces *Nodal* in the left LPM

Initially, *Car* transcripts are symmetrically detected in the hypoblast sheet of stage XII chick embryos. As gastrulation proceeds (with the appearance and subsequent elongation of the primitive streak), *Car* transcripts become more abundant, the higher concentration being detected at the anterior end of the mesendoderm layer (data not shown). By stage 4, *Car* is expressed bilaterally in the perinodal region of the embryo, before asymmetric expression of *Shh* or *ActRIIa* in Hensen's node is detected (Fig. 1a, a′). Subsequently, at stages 5 to 7–, and after the asymmetrical node distribution of *Shh* (in the left) and *ActRIIa* (in the right) are observed[1], *Car* is downregulated on the right side of the embryo (Fig. 1b, b′, c, c′). At stage 7, *Car* is expressed in the left paraxial mesoderm adjacent to the cells expressing *Shh* in the left side of the node (Fig. 1c shows a stage 7– embryo). A second domain of *Car* expression appears in the adjacent left LPM. Whereas the paraxial expression of *Car* disappears at around stage 8 (Fig. 1d), concomitantly with the disappearance of *Shh* expression in the adjacent cells[10], its expression domain in the left LPM expands both anteriorly and posteriorly. At stage 9, *Car* transcripts start to fade away from the left LPM (Fig. 1e), and by stage 10 they are undetectable. As the distribution of *Car* transcripts in the left LPM of stage 6–9 chick embryos appears to precede the onset of *Nodal* expression, we performed parallel whole-mount *in situ* hybridizations for *Nodal* and *Car* genes. *Nodal* transcripts, which are initially symmetrically distributed in the posterior two-thirds of the primitive streak and in immediately adjacent cells (Fig. 1f, f′), become asymmetrically expressed in the mesodermal cells abutting *Shh*-expressing cells in the node at stage 5+ (Fig. 1g, g′). At stage 7–, a second domain of *Nodal* expression appears in the left LPM (Fig. 1h, h′). Subsequent *Nodal* expression seems to follow the expansion of *Car* expression towards the head and anterior and caudal regions of the left LPM[1] (Fig. 1i, j).

The spatio-temporal pattern of *Car* expression indicates that *Car* may be the intermediary paraxial signal that transmits the Shh left–right positional information from the node (Fig. 2a) to the LPM in the chick embryo. Beads soaked in Shh were implanted on the right side of Hensen's node at stage 5, and whole-mount *in situ* hybridization for *Car* messenger RNA was performed at several timepoints thereafter. Ectopic induction (or maintenance) of *Car* expression was observed on the right LPM (in 18 out of 21 embryos; Fig. 2b). Also, left-sided treatment of stage 5 chick embryos with a blocking antibody that prevents Shh signalling[10] resulted in downregulation of *Car* expression (14/17 embryos; Fig. 2c). As with implantation of beads soaked in Shh, implantation of cell pellets expressing *Car*, or injection of a retroviral vector expressing the *Car* gene (*RCAS–Car*) on the right side of the node at stages 5–7 led to ectopic and broad induction of *Nodal* (58/85 embryos; Fig. 2d) and *Pitx2* (30/62 embryos; Fig. 2f, g), genes that are downstream targets of Shh signalling on the left. Ectopic *Car* expression also caused down-

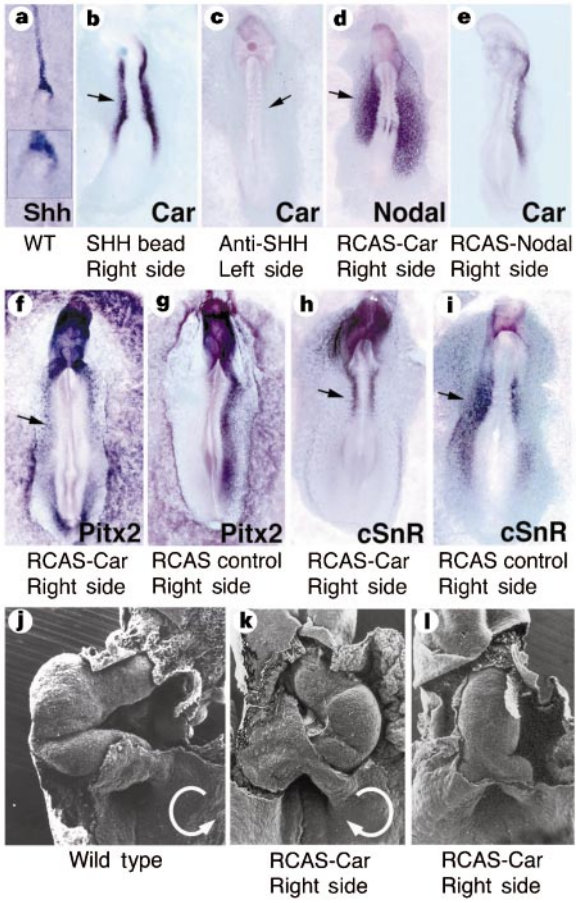

Figure 2 Car acts downstream of Shh and upstream of *Nodal* and directs heart looping in the chick embryo. The experimental manipulation and the site of the embryo where it was performed are indicated below each panel. The probes used for *in situ* hybridization are given in each panel. **a**, *Shh* is expressed asymmetrically in the left side of the node at stage 5+; inset, magnification of the node area. Stages of embryos shown in **b**–**i** are 9–12. **b**, A bead soaked in Shh protein was implanted on the right side of the chick Hensen's node at stage 5. This resulted in ectopic expression of *Car* in the right LPM (arrow). **c**, Implantation of a bead soaked in anti-Shh antibody on the left side of the node of stage 5 chick embryos downregulated the normal expression domain of *Car* in the left LPM (arrow). **d**, Injection of *RCAS–Car* on the right side of Hensen's node at stage 5 resulted in ectopic induction of *Nodal* transcripts (arrow). **e**, Injection of *RCAS–Nodal* on the right side did not affect expression of *Car*. **f**, **g**, Injection of *RCAS–Car* on the right side of Hensen's node at stage 5 induced ectopic expression of *Pitx2* (arrow in **f**). A control injection using *RCAS–alkaline phosphatase* did not affect *Pitx2* expression in the left LPM (**g**). **h**, **i**, Expression of *cSnr* in the right LPM (arrow in **i**) was downregulated by injection of *RCAS–Car* on the right side of Hensen's node at stage 5 (arrow in **h**). **j**–**l**, When embryos injected with the *RCAS–Car* construct on the right side of Hensen's node at stage 5 were allowed to develop until stages 12–13, about 50% of them had reversals of heart looping (**j**, **k**; white semicircular arrows indicate direction of heart looping). In a few cases the heart was bilaterally symmetric and heart looping did not seem to occur (**l**).

regulation of *cSnr*, a gene specifically expressed in the right LPM (16/24 embryos; Fig. 2h, i). Although misexpression of *Car* on the right side of the embryo induces *Nodal* expression, misexpression of *Nodal* did not induce *Car* expression (0/15 embryos; Fig. 2e). Finally, to ascertain whether the changes in gene expression elicited by ectopic expression of *Car* in the right LPM resulted in left–right morphological alterations, we implanted *Car*-expressing cells on the right side of chick embryos at stages 4–6 and scored for changes in heart morphology at stages 11–13 (Fig. 2j–l). As previously observed after *Shh* or *Nodal* misexpression, heart looping was randomized (9/21 embryos; Fig. 2j, k). In a few embryos, looping was arrested and the hearts appeared to be bilaterally symmetric (3/21 embryos; Fig. 2l). We conclude that expression of *Car* on the left side of the embryo plays an instructive role in determining heart *situs* and looping in the chick embryo.

Our results indicate that *Shh* is necessary and sufficient to induce and/or maintain *Car* expression, which acts upstream of *Nodal*. Together with the fact that proteins encoded by the *Cer/Dan* gene family are freely secreted into the extracellular medium[22,24,26,33], our data lead us to propose that Car, by acting as a long-range signal, fulfils all the requirements to be the factor that mediates the Shh-dependent induction of *Nodal* in the left LPM reported in the chick embryo.

Car induces *Nodal* by antagonizing BMPs

Cer-like secreted factors can antagonize BMP activity by binding directly to BMPs, thus blocking their interaction with BMP receptors[19,26,33]. Sequence analysis of the Cer-like protein Car shows that it contains the structural domain that mediates the interaction of Cer proteins with BMPs[33] (see below). Several BMPs are expressed in the LPM in bilaterally symmetrical patterns at the time at which *Nodal* expression appears in the left LPM[34–36] (for example, Fig. 3a shows a composite of *BMP-2* and *BMP-4* patterns). Around stage 7, *Nodal* expression is stronger in a subdomain that also expresses very high levels of *Car* (red asterisks in Fig. 3b, c). A more lateral subdomain of weaker *Nodal* expression abuts the region where *Car* transcripts are also more faintly expressed (green asterisks). Finally, *Nodal* is not detected in even more lateral regions where *BMP* transcripts (Fig. 3a) are present but *Car* is completely absent (yellow asterisks in Fig. 3a–c). As expected, after we implanted *Car*-expressing cells on the right side of the embryo, *Nodal* was induced in a high percentage of embryos (58/85 embryos; Fig. 3d, arrow). However, *Nodal* induction is observed much less frequently when a bead soaked in BMP is placed next to the *Car*-producing cells (only 3/34 embryos showed *Nodal* induction; Fig. 3e). Moreover, when a bead soaked in BMP is applied on the left side of the node, *Nodal* expression is downregulated (10/30 embryos; Fig. 3f, arrow). This indicates that Car and BMP have antagonistic effects on *Nodal* expression, and that Car might activate and/or maintain *Nodal* expression in the left LPM by antagonizing a repressive effect of BMP.

To validate this hypothesis independently *in vivo*, we used Noggin, a secreted factor structurally unrelated to Car that can bind BMPs[37] and antagonize their activities[37–39]. We misexpressed Noggin on the right side of the node at stages 4–5 either by implanting a pellet of *Noggin*-expressing cells or by infecting embryos with *RCAS–Noggin*[38]. This resulted in induction of *Nodal* expression (Fig. 3g). We confirmed that Car itself may act as a BMP antagonist by performing two different assays in chick embryos, where antagonism of BMP activity is well characterized (see Supplementary Information). First, Car can abolish formation of cartilage nodules in micromass cultures of limb mesenchymal cells, and this effect can be rescued by adding BMP protein. Second, *Car* misexpression in chick limbs has the same effect as *Noggin* misexpression[38].

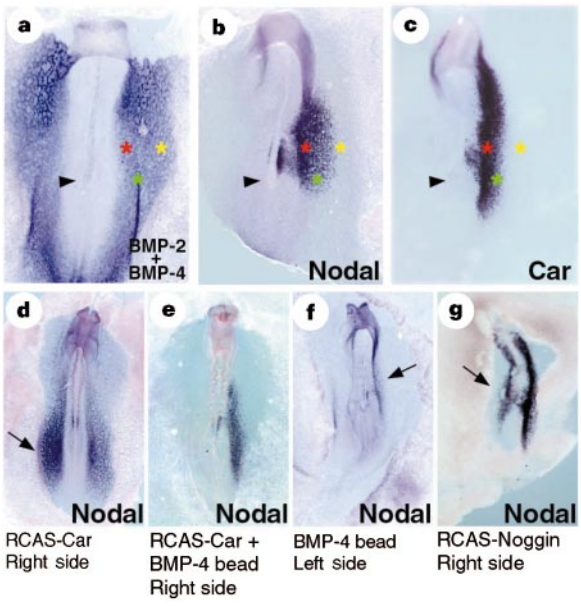

Figure 3 Antagonism of BMPs by Car regulates *Nodal* expression. **a**, The sum of the expression patterns of *BMP-2* and *BMP-4* in a stage 7 embryo reveals that *BMP*s are expressed in broad symmetrical domains in the left and right LPM. **b**, **c**, *Nodal* expression in the LPM at the same stage is restricted to the left side, where *Car* (**c**) is also expressed. *Nodal* expression is stronger in the region that also expresses very high levels of *Car* (red asterisks in **a**–**c**). Green asterisks mark a more lateral subdomain of weaker *Nodal* expression (**b**) that overlaps the region where *Car* transcripts are also more weakly expressed (**c**). *Nodal* is absent from the regions indicated by yellow asterisks, where *BMPs* are present but *Car* is completely absent. Arrowheads in **a**–**c** point to the node. **d**, When *Car*-expressing cells (*RCAS–Car*) were implanted on the right side of Hensen's node at stage 5, *Nodal* was ectopically induced (arrow). **e**, Induction of *Nodal* was much less frequent when a bead soaked in BMP-4 (1 mg ml^{-1}) was implanted with a graft of *Car*-expressing cells (**e** shows an embryo where induction of *Nodal* by *Car* on the right side has been completely inhibited). **f**, When a bead soaked in BMP-4 (1 mg ml^{-1}) is applied on the left side of the node at stage 4, *Nodal* expression in the left LPM is strongly downregulated (arrow). **g**, When cells expressing the BMP antagonist Noggin are implanted on the right side of the node at stage 5, *Nodal* is ectopically induced (arrow).

Interaction of Car with BMPs and Nodal

To test for a possible direct interaction between Car and BMPs, we produced in COS7 cells a triple myc-epitope-tagged version of Car (Car–myc3), and tested by immunoprecipitation its possible interactions with several members of the TGF-β superfamily, including BMP-4, BMP-5, Nodal, GDF-5 and Activin (Fig. 4a; see Methods). When COS7-conditioned medium containing Car–myc3 was incubated with BMP-4, immunoprecipitation with an anti-myc antibody pulled down BMP-4, as detected by western blotting using an antibody against BMP-4. Similarly, when conditioned medium containing Car–myc3 was incubated with ^{35}S–Nodal, immunoprecipitation with an anti-myc antibody pulled down ^{35}S–Nodal. When similar experiments were performed with BMP-5, a tagged version of GDF-5 (GDF-5–Flag) or Activin, these proteins were not pulled down by immunoprecipitation with the anti-myc antibody. We conclude that Car interacts specifically with certain members of the TGF-β superfamily (BMP-4 and Nodal). Similar results have been obtained for the *Xenopus* Cer protein, which also binds BMP-4 and Nodal but not Activin[33]. In our experimental setting, the Car–Nodal interaction is reduced by about 50% when human Cer is included in the binding reaction (Fig. 4a).

We also performed sequence analysis and modelling to gain insight into the structural basis for the antagonistic interaction between Cer-like and BMP-like proteins. A multiple sequence alignment (MSA) with CLUSTALX[40] of the cysteine-rich region of several Cer-like proteins, together with BMPs and Nodals, reveals two distinct groups with different sequence patterns (Fig. 4b). A Cer-like group, that we shall call β-like, is characterized by a C-

terminal cysteine knot, and has two cysteine residues at positions 15 and 83, together with a short deletion in positions 41–44 and 57–64, as hallmarks (Fig. 4b). BMP-like proteins, which we shall describe as α-like, show a TGF-β2-like pattern with a characteristic α-helix between positions 48–54 (Fig. 4b).

A survey of the structural classification of proteins (SCOP) database reveals an example of an interaction between a β-like and an α-like sequence: the heterodimeric (α and β) structure of human chorionic gonadotropin. This indicates that the interaction between Cer-like and BMP-like proteins could be reminiscent of the gonadotropin mode of interaction. This structural inference is supported by sequence analysis. After incorporation of the human gonadotropin sequences in the MSA of Cer-like and BMP-like sequences, followed by further clustering, we found that the β-chain is more similar to Cer-like sequences than to the α-chain, which is more similar to BMP-like sequences (Fig. 4b). The available information, both from the sequence analysis and the structural model, indicates a mode of interaction between BMP-like and Cer-

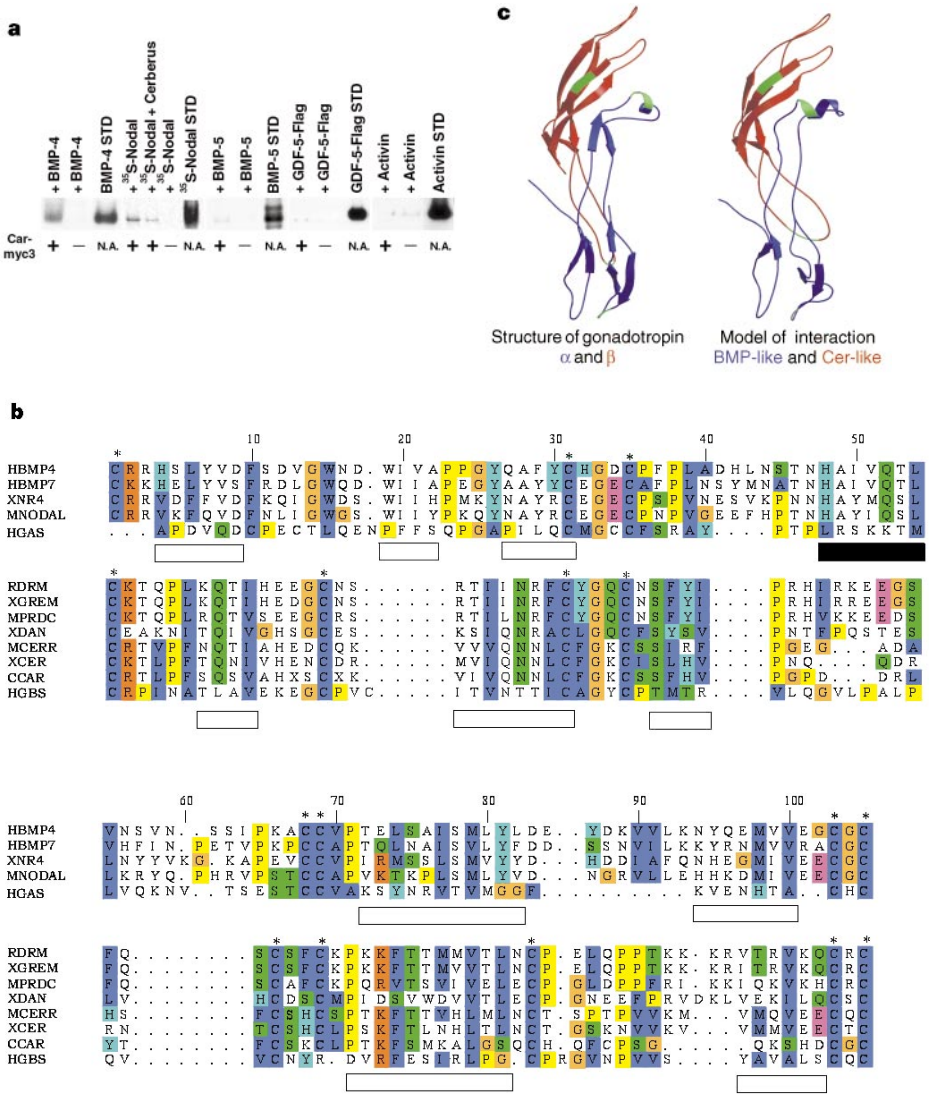

Figure 4 Interaction of Car with BMPs: biochemical evidence and structural model. **a**, COS7-conditioned medium containing Car–myc3 was incubated with several TGF-β proteins (see Methods), and an anti-myc antibody was used to immunoprecipitate Car–myc3 and associated proteins, which were then detected either by phosphoimaging (^{35}S–m Nodal) or by western blotting using antibodies against the corresponding proteins or their epitope tags. Car–myc3 binds to BMP-4 and Nodal but not to other TGF-βs such as BMP-5, GDF-5 and Activin. Human Cerberus competes with Car–myc3 for binding to Nodal (**a**). The lanes marked STD refer to independent assays performed with the same batches of proteins used for the experiments involving Car–myc3, which confirm that all the proteins used were biochemically active in the immunoprecipitation assay. N.A., not applicable: those independent assays do not involve Car–myc3 (details available upon request). **b**, MSA of selected cysteine-rich regions of the BMP-like proteins human BMP-4 (HBMP4), human BMP-7 (HBMP7), *Xenopus* Nodal related (XNR4) and mouse Nodal (MNODAL), aligned to the cysteine-rich region of the human gonadotropin α-subunit (HGAS); and of cysteine-rich regions of the Cer-like proteins rat-DRM (RDRM), *Xenopus* Gremlin (XGREM), mouse PRDC (MPRDC), *Xenopus* Dan (XDAN), mouse Cer-related (MCERR), *Xenopus* Cerberus (XCER) and chicken Caronte (CCAR), aligned to the cysteine-rich region of the human Gonadotropin β subunit (HGBS). The MSA was made using ClustalX[40]. Colours indicate conserved properties. Consensus secondary structure prediction is depicted by open (β-strand) or filled (α-helix) rectangles below the alignments. Asterisks denote conserved cysteine residues inside each group. **c**, Model of interaction between BMP-like and Cer-like cysteine-rich regions. Left, ribbon diagram of the structure of the α- (blue) and β-chains (red) of the human gonadotropin hormone. Right, model by homology using MODELLER (details available upon request) of the cysteine-rich region of human BMP-4 (blue) and chicken Car (red). Green, key residues unmasked by a Factor Analysis (FA). In both cases, they cluster around the α-helix and the loop between the last two β strands in the blue chains and around the second β-like gonadotropin sequences. A similar situation is observed for the BMP-like sequences, where the residues detected are equivalent to those observed if the α-like gonadotropin sequences are used. Mapping these residues, respectively, onto the structure of the α- and β-chains of the human gonadotropin (left) or onto a homology model of the interaction between BMP-like and Cer-like sequences based on the previous structure (right), shows that they appear at the interface between chains that correspond to the functional areas of the complex.

like proteins similar to that observed between the α- and β-chains of the human gonadotropin (Fig. 4c).

As Car seems to be a multifunctional antagonist, able to bind BMP and Nodal proteins, the question arises of why the presence of Car in the left LPM does not interfere with Nodal activity. As a result of Car antagonizing BMP activity in the LPM, *Nodal* transcripts begin to accumulate quickly at stage 7 and reach high levels throughout the left LPM at a time at which an accumulation of Nodal protein can presumably overcome the antagonism by Car. Thus it is unlikely that Car significantly interferes with the activation of Nodal transcriptional targets (such as *Pitx2*) at that stage of development. Consistent with this interpretation, when we deliver Car to the left side of the embryo by implanting *Car*-producing cell grafts, *Nodal* transcription is strongly upregulated, even outside its normal domain of expression (data not shown).

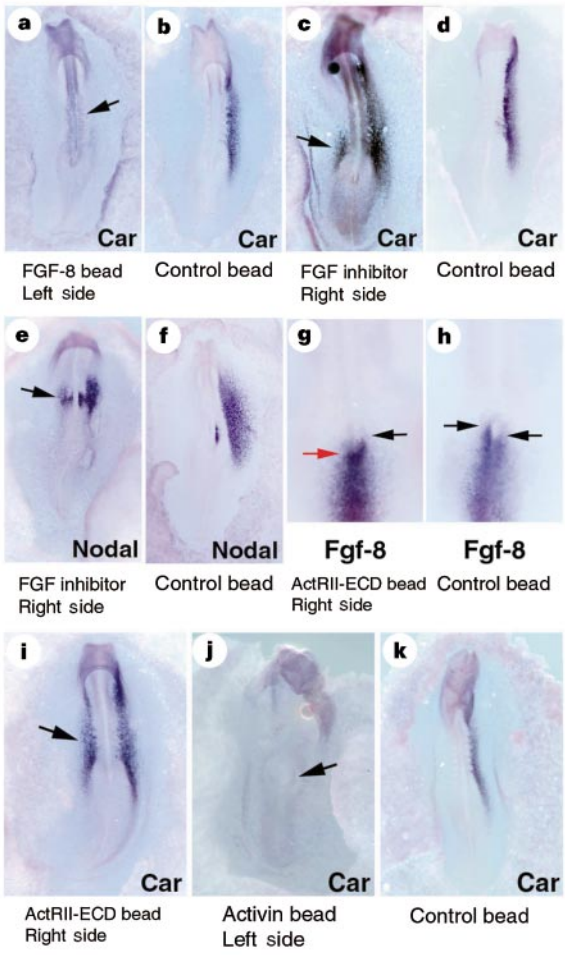

Figure 5 FGF-8 and Activin regulate *Car* expression. The embryos shown in **a**–**d** and **i**–**k** are stages 7–9. **a**, When a bead soaked in FGF-8 protein (1 mg ml^{-1}) was implanted on the left side of Hensen's node at stage 5, *Car* transcripts were downregulated (arrow). **b**, *Car* expression was not affected by control BSA-soaked beads. **c**, Inhibition of FGF signalling by application of SU5402 (1 mg ml^{-1}) to the right side of Hensen's node at stage 5 maintained and/or induced *Car* expression (arrow). **d**, Normal *Car* expression when BSA control beads were applied. **e**, A bead soaked in SU5402 implanted on the right side of Hensen's node at stage 5 induced ectopic expression of *Nodal* on the right side (arrow). **f**, Control beads had no effect on *Nodal* expression (slightly older embryo). **g**, Stage 6 embryo. During normal development, *FGF-8* is expressed in the right but not left posterior portion of the node. When a bead soaked in the truncated Activin receptor (ActRII–ECD) (0.5 mg ml^{-1}) was applied to the right side of Hensen's node at stage 4, the right-sided *FGF-8* expression in the node was downregulated (red arrow). Black arrow, normal anterior level of *FGF-8* on the left side of the node. **h**, Stage 6 embryo. Control beads had no effect on normal expression of *FGF-8* in the right posterior portion of the node (arrows). **i**, A bead soaked in ActRII–ECD (0.5 mg ml^{-1}) applied to the right side of the node at stage 4 maintained and/or induced *Car* expression on the right side (arrow). **j**, Application of a bead soaked in Activin (0.5 mg ml^{-1}) on the left side of the node at stage 4 downregulated expression of *Car* in the left LPM (arrow). **k**, BSA control beads did not affect *Car* expression.

Regulation of *Car* expression by FGF-8

Downregulation of *Car* expression on the right side of the embryo is essential for normal left–right development, as ectopic presence of *Car* on the right side results in laterality defects. A good candidate for repressing *Car* on the right side of the embryo is FGF-8. The *FGF-8* gene begins to be expressed asymmetrically in the node under the control of Activin βB[14] around the time when *Car* is downregulated on the right side of the embryo. Moreover, ectopic application of FGF-8 protein inhibits the expression of the left-specific genes *Nodal* and *Pitx2*, and induces expression of the right-specific gene *cSnR* when applied to the left side of the embryo[14]. Beads soaked in FGF-8 implanted in the left side of the node at stage 5 downregulate *Car* transcripts (8/20 embryos; Fig. 5a, b). To further substantiate the role of FGF-8 as a repressor of *Car*, we inhibited FGF signalling in two ways. First, when beads soaked in the FGF receptor-1 (FGFR-1) inhibitor SU5402 (ref. 41) were applied to the right side of the node, *Car* expression was maintained and/or induced (5/20 embryos; Fig. 5c, d), and *Nodal* was ectopically expressed on the right side (6/22 embryos; Fig. 5e, f. The embryo in 5f is older than that in 5e). Second, we repeated the experiment using beads soaked in a soluble version of a truncated Activin receptor (ActRII-ECD) that specifically inhibits Activin signalling[16]. This resulted in the downregulation of *FGF-8* expression on the right posterior side of the node (9/15 embryos; red arrow in Fig. 5g, compare with 5h) and maintenance and/or induction of *Car* expression on the right LPM (9/19 embryos; Fig. 5i). Conversely, implantation of Activin on the left side of the embryo led to a downregulation of *Car* expression in the left LPM (12/18 embryos; Fig. 5j, k).

Our results are compatible with *FGF-8* expression on the right side of the node acting as a negative regulator of *Car* expression. Thus, *Car* is activated (or maintained) by *Shh* in the left side of the embryo and repressed by *FGF-8* in the right side. This ensures that by stage 6 *Car* transcription is restricted to the left side of the gastrulating chick embryo.

Lefty-1 stabilizes asymmetric gene expression

The *Lefty-1* gene has been proposed to be vital for restricting the expression of *Nodal*, *Lefty-2* and *Pitx2* to the left side of the embryo, acting as (or inducing) a 'midline barrier' that would prevent the presence of the 'X' factor on the right side of the embryo[12,13]. We have investigated the role of Lefty-1 in left–right determination in the chick, and its possible interaction with *Car*.

Lefty-1 appears earlier in the chick than in the mouse embryo. In the mouse, *Lefty-1* is expressed predominantly in the presumptive floorplate, beginning at the two-somite-pair stage[30]. In the chick, *Lefty-1* transcripts are detected in Koller's sickle at the posterior margin of the chick blastoderm at stages X–XII (data not shown) in cells that will later contribute to Hensen's node, the chick organizer[42]. Subsequently, as the primitive streak elongates, *Lefty-1* transcripts become restricted to the anterior half of the streak (Fig. 1k, k′). At stage 5+, *Lefty-1* transcripts are observed in a pattern overlapping the domain of *Shh* expression on the left side of the node (Fig. 1l, l′, compare with *Shh* in Fig. 2a). From stages 6 to 8, *Lefty-1* expression is restricted to the left side of the prechordal mesoderm, and by stage 8, coinciding with the disappearance of the left-sided *Shh* expression, *Lefty-1* becomes symmetrically distributed throughout the caudal notochord (Fig. 1n; 1n′ is a section of the embryo shown in 1o). Before *Lefty-1* is no longer detectable at stage 11, a small domain of expression is observed in the left posterior LPM overlapping the *Nodal*-expressing cells (Fig. 1o, compare with 1j).

When either cells expressing mouse *Lefty-1* or an *RCAS* virus containing the mouse *Lefty-1* gene were applied at stages 4–5 to the right side of the node, we observed repression of both *FGF-8* (8/15 embryos; Fig. 6a, b) and *cSnR* (8/20 embryos; Fig. 6f), and activation of left-specific genes such as *Car* (8/15 embryos; Fig. 6c), *Nodal* (9/18 embryos; Fig. 6d) and *Pitx2* (10/25 embryos; Fig. 6e). These results, together with those shown in Fig. 5, lead us to propose that Lefty-1 might be able to antagonize Activin. Several plausible mechanisms can be envisioned, including competitive binding of Lefty-1 to the Activin receptor, which would result in an inactive ligand–receptor complex that would not be able to induce *FGF-8* on the right side of the node. A similar role in inactivating Activin pathways has been proposed for Antivin, whose function in zebrafish can be substituted by mouse *Lefty-1* (ref. 29). These results indicate that the early domain of expression of *Lefty-1* in the left side of the embryo (adjacent to the node) is important as a safety mechanism that ensures that the Activin pathway is completely inactive on the left side of the embryo, allowing continued expression of left-specific genes such as *Car*, *Nodal* and *Pitx2*.

An excess of mouse Lefty-1 on the left side of the chick node blocks activation of *Nodal* expression in the left LPM[13]. Here we show that, although expression of *Nodal* is either absent or downregulated after application of mouse Lefty-1 on the left side of the stage-5 chick node (9/15 embryos; Fig. 6h), *Car* expression is not affected (0/15 embryos; Fig. 6g). As we have shown that *Car* is necessary and sufficient to activate *Nodal*, these results indicate that Lefty-1 may antagonize Car activity without affecting its transcription. One possibility is that Lefty-1 could antagonize Car activity by binding to it. In doing so, Lefty-1 would limit Car diffusion and would effectively interfere with its function. This assumption goes along with the hypothesis that the expression of Lefty-1 on the left side of the node and on the left side of the midline could serve as a barrier to prevent spreading of Car (or, in general terms, the *Shh-*

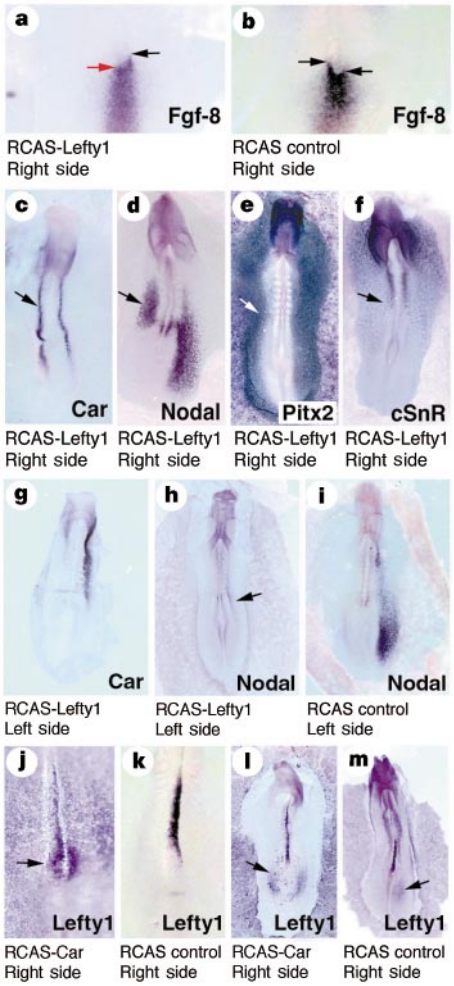

Figure 6 Interaction between *Lefty-1* and *Car* during the establishment of left–right asymmetry. **a**, Stage 6 embryo. When cells expressing mouse *Lefty-1* (*RCAS–Lefty-1*) were implanted on the right side of Hensen's node at stage 4, the right-sided *FGF-8* expression in the node was downregulated (red arrow). Black arrow, normal anterior *FGF-8* expression on the left side of the node. **b**, Stage 6 embryo. Control cells expressing *alkaline phosphatase* had no effect on the expression of *FGF-8* in the right posterior portion of the node (arrows). Embryos in **c**–**i** are at stages 8–10. **c**–**e**, A retrovirus vector containing the mouse *Lefty-1* gene was injected at stage 4 to the right side of the node, producing ectopic induction of *Car* (arrow in **c**), *Nodal* (arrow in **d**) and *Pitx2* (arrow in **e**). **f**, The normal expression domain of *cSnR* in the right LPM was downregulated by injection of RCAS–*Lefty-1* at stage 4 on the right side of the node (arrow). **g**, *RCAS–Lefty-1* on the left side of Hensen's node at stage 4 did not affect the normal expression of *Car* in the left LPM. **h**, The same experiment downregulated *Nodal* expression (arrow). **i**, The control virus (*RCAS–alkaline phosphatase*) had no effect on *Nodal* expression. **j**–**m**, When a graft of *Car*-expressing cells (indicated as *RCAS–Car*) was implanted on the right side of Hensen's node at stage 4, *Lefty-1* expression was upregulated on the right side of the node (arrow in **j**; compare with control in **k**). Infection with *RCAS–Car* produced upregulation of *Lefty-1* on the posterior side of the right LPM (arrow in **l**; compare with the control experiment in **m**, where normal expression in the left LPM is indicated by an arrow).

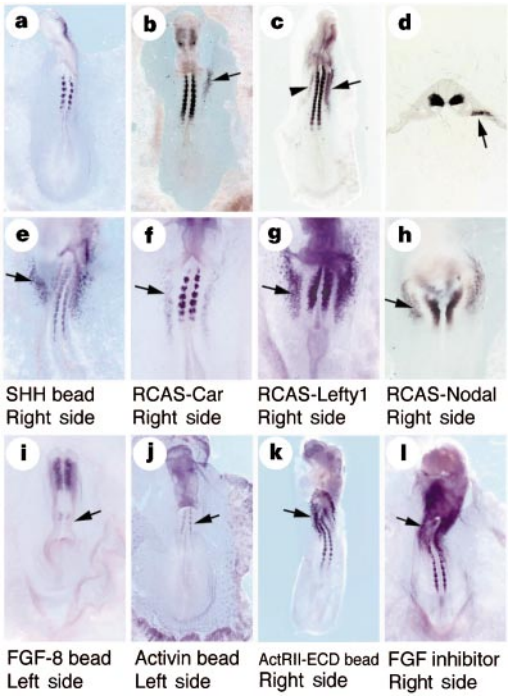

Figure 7 *cNKX3.2* is a novel target of the left–right signalling pathway. **a**, Expression of the *cNKX3.2* gene in somites at stage 8. **b**, At stage 10, transcripts are still detected in the somites and two new domains of expression are observed in the head mesoderm and the left LPM (arrow). **c**, As well as the head mesoderm, somites and left LPM (arrow), a faint expression domain is now observed in the right LPM (arrowhead). **d**, Cross-section (at the level of the arrow) of the embryo shown in **b** displaying symmetrical expression of *cNKX3.2* in the somites and left-specific staining in the LPM (arrow). **e**–**h**, Application of beads soaked in Shh protein (**e**) and *RCAS–Car* (**f**), *RCAS–Lefty-1* (**g**) or *RCAS–Nodal* (**h**) viruses to the right side of the Hensen's node at stage 5 induced ectopic expression of *cNKX3.2* in the right LPM (arrows). **i**, Implantation of a bead soaked in FGF-8 (1 mg ml^{-1}) on the left side of Hensen's node at stage 5 downregulated expression of *cNKX3.2* in the left LPM and somites (arrow). **j**, Application of a bead soaked in Activin (1 mg ml^{-1}) on the left side of Hensen's node at stage 5 downregulated expression of *cNKX3.2* in the left LPM and somites (arrow). **k**, Application of the truncated activin receptor ActRII-ECD (0.5 mg ml^{-1}) to the right side of Hensen's node at stage 5 enhanced expression of *cNKX3.2* in the right LPM (arrow). **l**, A similar result (arrow) was obtained when the FGFR-1 inhibitor SU5402 (1 mg ml^{-1}) was applied to the right side of the embryo.

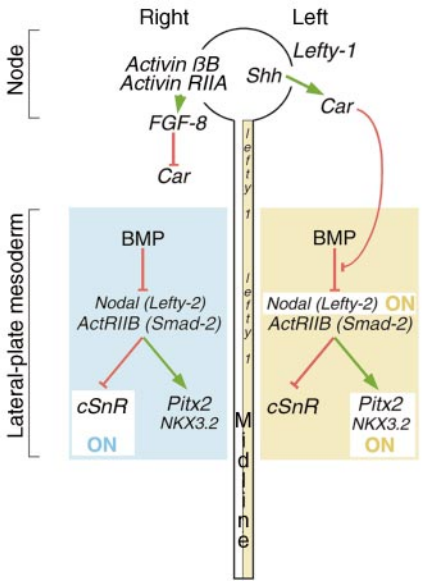

Figure 8 Role of *Car* in the genetic cascade that determines left–right development. Control of *Car* expression by *Shh* and FGF-8, together with a possible barrier mechanism elicited by Lefty-1, restricts Car activity to the left side of the embryo, where it can antagonize the repressive effect of BMPs on *Nodal* transcription. *Nodal* activates downstream left-specific genes and represses right-specific genes in the LPM. Green arrows indicate activation and red lines indicate repression; in the case of Car the red line indicates antagonism of BMPs by direct binding to them. It cannot be ruled out that a factor other than Car might actually be the 'X' factor that diffuses to the right (or is transcribed on the right) in the absence of *Lefty-1*, according to the barrier model[18]. However, as Car fulfils all the required criteria to be the 'X' factor, even if that additional factor exists, it probably acts through *Car* or in a pathway related to *Car*. A better understanding of the role of the *Car* gene in left–right development must await its identification and ablation in the mouse. This is a simplified model intended to illustrate the role of *Car*, and only some of the genes involved in left–right development are included.

dependent 'X' factor) from the left to the right side of the embryo. Alternatively, Lefty-1 might repress *Nodal* transcription by mechanisms unrelated to Car. An added twist is that Lefty proteins seem to be able to antagonize Nodal activity by mechanisms that could involve either competition with Nodal for a common receptor, formation of inactive heterodimers with Nodal or both. Identification of the murine Car and analysis of its pattern of expression in wild-type and *Lefty-1*$^{-/-}$ mice will be necessary to determine the nature of the regulatory relationship between *Car* and *Lefty-1*. *Car*-expressing cells implanted on the right side of the embryo can induce expression of *Lefty-1* on the right side of the midline (8/15 embryos; Fig. 6j, k) and in the right LPM (7/15 embryos; Fig. 6l, m). As Car presumably acts as an extracellular antagonist, it might induce *Lefty-1* in the midline by antagonizing a repressive activity of some TGF-β member on *Lefty-1* transcription. *BMPs* are expressed along the primitive streak and are likely candidates to encode this repressive activity. Of course, additional regulators may control *Lefty-1* expression, as even ectopic expression induced by *Car* is similar to the endogenous pattern observed on the left side of the embryo.

cNKX3.2 is a target of the left–right pathway

Finally, we have identified the homeobox gene *cNKX3.2*, which is the chick homologue of mouse *BapX1/NKX3.2* (ref. 43); the same gene was independently isolated by another group[32]. *NKX* genes are involved in cellular differentiation and organogenesis in different organisms[44,45]. *cNKX3.2* begins to be expressed at stages 8–9, where it is observed in the somites (Fig. 7a). At stages 10–11, *cNKX3.2* appears in the head mesoderm and in the left LPM (Fig. 7b, d). Around stage 14, faint expression is also seen in the right LPM (Fig. 7c). At later stages *cNKX3.2* is expressed in other embryonic structures, including gut and limbs (data not shown), with a very similar pattern to that reported for its mouse and *Xenopus* orthologues.

We decided to investigate in detail the mechanisms that regulate *cNKX3.2* transcription, in order to place it in the genetic cascade that controls left–right asymmetry. Misexpression of either Shh (16/18 embryos; Fig. 7e), *Car* (19/28 embryos; Fig. 7f), mouse *Lefty-1* (12/28 embryos; Fig. 7g) or *Nodal* (14/30 embryos; Fig. 7h) in the right side of the embryo all induce strong *cNKX3.2* expression in the right LPM. Conversely, misexpression of either FGF-8 (11/18 embryos; Fig. 7i) or Activin (8/17 embryos; Fig. 7j) in the left side of the embryo inhibits the normal domain of *cNKX3.2* expression. We confirmed the specificity of the effect of these two right signals by misexpressing either a soluble version of a truncated Activin receptor (which inhibits activin signalling; 8/23 embryo; Fig. 7k) or the specific FGFR-1 inhibitor SU5402 (6/19 embryos; Fig. 7l) on the right side of the embryo. Both manipulations induce *cNKX3.2* expression in the right LPM. In general, *cNKX3.2* responds to upstream left–right signals in a similar way to *Pitx2*. Like *Pitx2*, we consider *cNKX3.2* to be a target of the early patterning network of left–right signals involved in executing the cellular changes that are responsible for organ morphogenesis.

It is debatable whether a general mechanism of left–right determination (Fig. 8) applies to all vertebrates. Although the left-specific expression of important determinants such as *Nodal* and *Pitx2* seems to be conserved in all vertebrates examined so far, this may not be the case for upstream regulators. For example, expression of *Shh* and *FGF-8* has not been reported to be asymmetric in *Xenopus* or mouse. However, *Shh*$^{-/-}$ and *FGF-8*$^{-/-}$ mutants show laterality defects, including altered expression of *Nodal*, *Pitx2* and *Lefty-2* (refs 46–48). In the mouse, *Shh* seems to be required to induce and/or maintain the midline barrier that has been proposed to restrict expression of *Nodal*, *Lefty-2* and *Pitx2* to the left side of the embryo[12,13]. In this model, *Shh* would not be required for left-sided expression of these genes. This interpretation contrasts with its proposed role as a left determinant in the chick. A more accurate assessment of the degree of evolutionary conservation of left–right determination mechanisms awaits a future analysis of the roles of *Shh*, *FGF-8* and other genes involved in left–right development in different organisms; thus extending the analysis of the network of molecular interactions described here to other vertebrates should provide further insight into the general mechanisms of left–right determination. □

Methods

Cloning of *Car*, *Lefty-1* and *cNKX3.2*

Left and right LPM mRNAs from embryos at stages 6–12 were isolated using standard protocols. A left LPM substracted complementary DNA library was obtained using the Clontech PCR-Select cDNA substraction kit. Seventy clones were selected at random and used to generate digoxigenin-labelled probes. After confirming that three of the clones represented differentially expressed genes, we sequenced them in both strands. The *Lefty-1* fragment was isolated indirectly from the PCR-Select differential screening and used to screen a chick genomic library to obtain the full-length *Lefty-1* gene using standard protocols. The *Car* and *cNKX3.2* full-length clones were obtained by screening stage 5 and 12 chick cDNA libraries, respectively, with noncoding fragments isolated from the PCR-Select differential screening (for *Car*) and by using a 5′ RACE-Smart kit from Clontech (for *cNKX3.2*). The chick *Car*, *cNKX3.2* and *Lefty-1* sequences have been deposited in GenBank under accession numbers AF179484, AF179482 and AF179483, respectively.

Retroviral infection and bead implantation

Chick embryos were explanted and grown *in vitro* as described[49]. *RCAS* (subtype A) retroviral stocks containing full-length *Car*, *Nodal*, mouse *Lefty-1* and *alkaline phosphatase* (used as control) were produced as described[16]. Embryos were either infected with *RCAS* viruses by air pressure and/or grafted with *RCAS*-infected cells on either side of the chick blastoderm near Hensen's node. Beads were soaked in Shh protein, anti-Shh antibody and FGF as described[10]. The FGFR1 inhibitor SU5402 (ref. 41; CalBiochem) was used at 1 mg ml^{-1}.

In situ hybridization

After viral infection and/or bead implantation, we processed embryos for whole-mount *in situ* hybridization as described[42]. Sectioning of stained embryos was as described[16].

Antisense probes for *Car* and *cNKX3.2* spanned the entire open reading frame (ORF). For *Lefty-1* we used the entire isolated fragment. We generated a 450-base-pair (bp) probe corresponding to the 3′ untranslated region that gave an identical pattern of expression to that obtained with the cDNA fragment (data not shown). The rest of the probes were produced as described[16].

Co-immunoprecipitation experiments

A triple myc-tagged version of Car (Car–myc3) was obtained by cloning a *Car* insert into the mammalian expression vector pMT21-myc3, bringing the *Car* ORF without a stop codon in frame with a triple myc-tag (5′-GAG CAG AAG CTG ATA TCC GAA GAA GAC CTC GGC GGA GAG CAG AAG CTC ATA AGT GAG GAA GAC TTG GGC GGA GAG CAG AAG CTT ATA TCC GAA GAA GAT CTC GGA CCG TGA TAA-3′). The construct was verified by restriction analysis and dideoxy sequencing. Conditioned media from COS7 cells transfected with the pMT21–Car–myc3 construct was obtained using standard protocols. Briefly, serum-free conditioned media were collected two days after the start of transfection, cleared of cell debris and made up to 5 mM EDTA. Conditioned media were stored at 4 °C. The expression of Car–myc3 was verified by western blotting for the *myc* epitope. Under nonreducing conditions, Car–myc3 had a relative molecular mass of ~40,000, consistent with the predicted molecular mass of Car–myc3 and accounting for glycosylation at two potential N-linked glycosylation sites. Dimeric and multimeric forms of Car–myc3 were also observed, as seen for other members of the Cer/Dan family of BMP antagonists (A. N. Economides and N. Stahl, unpublished results). A similar procedure was used to obtain conditioned medium containing human GDF-5–Flag[50]. Car–myc3 (1 ml of COS7-derived serum-free conditioned medium) was incubated with human BMP-4 (0.5 $\mu g\,ml^{-1}$; R&D Systems), human BMP-5 (0.5 $\mu g\,ml^{-1}$; R&D Systems), human GDF-5–Flag (0.2 ml COS7-derived conditioned medium) or mouse Nodal (mBMP-16; provided as ^{35}S–mNodal expressed in *Xenopus laevis* oocytes). The formation of a stable complex between Car–myc3 and these different TGF-βs was determined by immunoprecipitating Car–myc3 and associated proteins using an anti-myc monoclonal antibody (9E10; 1 $\mu g\,ml^{-1}$) bound to Protein A-Ultralink (Pierce). The binding reaction was carried out in serum-free conditioned medium after it was made 20 mM Tris, pH 7.6, 150 mM NaCl, 0.1% Tween 20 (TBST), by addition of a 10× concentrate of these reagents. Binding was allowed to proceed for 1 h at 25 °C in a reaction volume of 1.1 ml, with continuous mixing to keep the Protein A-Ultralink (20 μl bead volume) in suspension, after which point the beads were spun down, washed once with TBST, transferred to new eppendorf tubes and washed three more items with TBST. Proteins bound to the beads were solubilized by addition of 25 μl of Laemmli SDS-PAGE sample buffer and loaded onto 4–12% NuPAGE/MES gradient gels (Novex), which were run under reducing conditions. The proteins were subsequently transferred onto Immobilon P and western blotted to detect human BMP-4, human BMP-5 or human Activin using antisera raised against the respective proteins (R&D Systems). In the case of human GDF-5–Flag, we used a monoclonal antibody raised against the Flag tag (M2; Kodak). ^{35}S–mNodal was visualized using a Phosphorimager (Fuji). None of the TGF-β proteins tested binds to the beads when Car–myc3 is excluded from the reaction mixture and instead substituted with COS7-derived conditioned medium from cells that had been transfected with a pMT21 plasmid.

Received 22 June; accepted 17 August 1999.

1. Levin, M., Johnson, R. L., Stern, C. D., Kuehn, M. & Tabin, C. A molecular pathway determining left-right asymmetry in chick embryogenesis. *Cell* **82,** 803–814 (1995).
2. Harvey, R. P. Links in the left/right axial pathway. *Cell* **94,** 273–276 (1998).
3. Ramsdell, A. F. & Yost, H. J. Molecular mechanisms of vertebrate left-right development. *Trends Genet.* **14,** 459–465 (1998).
4. King, T. & Brown, N. A. Embryonic asymmetry: the left side gets all the best genes. *Curr. Biol.* **9,** R18–R22 (1999).
5. Collignon, J., Varlet, I. & Robertson, E. J. Relationship between asymmetric *nodal* expression and the direction of embryonic turning. *Nature* **381,** 155–158 (1996).
6. Lowe, L. A. *et al.* Conserved left-right asymmetry of nodal expression and alterations in murine *situs inversus*. *Nature* **381,** 158–161 (1996).
7. Supp, D. M., Witte, D. P., Potter, S. S. & Brueckner, M. Mutation of an axonemal dynein affects left-right asymmetry in inversus viscerum mice. *Nature* **389,** 963–966 (1997).
8. Hyatt, B. A., Lohr, J. L. & Yost, H. J. Initiation of vertebrate left-right axis formation by maternal vg1. *Nature* **384,** 62–65 (1996).
9. Lohr, J. L., Danos, M. C. & Yost, H. J. Left-right asymmetry of a *nodal*-related gene is regulated by dorsoanterior midline structures during *Xenopus* development. *Development* **124,** 1465–1472 (1997).
10. Pagán-Westphal, S. M. & Tabin, C. J. The transfer of left-right positional information during chick embryogenesis. *Cell* **93,** 25–35 (1998).
11. Levin, M., Roberts, D. J., Holmes, L. B. & Tabin, C. Laterality defects in conjoined twins. *Nature* **384,** 321 (1996).
12. Meno, C. *et al.* Lefty-1 is required for left-right determination as a regulator of Lefty-2 and Nodal. *Cell* **94,** 287–297 (1998).
13. Yoshioka, H. *et al. Pitx2*, a bicoid-type homeobox gene, is involved in a lefty-signaling pathway in determination of left-right asymmetry. *Cell* **94,** 299–305 (1998).
14. Boettger, T., Wittler, L. & Kessel, M. FGF8 functions in the specification of the right body side of the chick. *Curr. Biol.* **9,** 277–280 (1999).
15. Isaac, A., Sargent, M. G. & Cooke, J. Control of vertebrate left-right asymmetry by a Snail-related zinc finger gene. *Science* **275,** 1301–1304 (1997).
16. Ryan, A. K. *et al.* Pitx2 determines left-right asymmetry of internal organs in vertebrates. *Nature* **394,** 545–551 (1998).
17. Campione, M. *et al.* The homeobox gene *Pitx2*: mediator of asymmetric left-right signaling in vertebrate heart and gut looping. *Development* **126,** 1225–1234 (1999).
18. Bouwmeester, T., Kim, S. H., Sasai, Y., Lu, B. & De Robertis, E. M. Cerberus is a head-inducing secreted factor expressed in the anterior endoderm of Spemann's organizer. *Nature* **382,** 595–601 (1996).
19. Hsu, D. R., Economides, A. N., Wang, X., Eimon, P. M. & Harland, R. M. The *Xenopus* dorsalizing factor Gremlin identifies a novel family of secreted proteins that antagonize BMP activities. *Mol. Cell* **1,** 673–683 (1998).
20. Ozaki, T. & Sakiyama, S. Molecular cloning and characterization of a cDNA showing negative regulation in v-src-transformed 3Y1 rat fibroblasts. *Proc. Natl Acad. Sci. USA* **90,** 2593–2597 (1993).
21. Stanley, E. *et al.* Dan is a secreted glycoprotein related to *Xenopus* cerebus. *Mech. Dev.* **77,** 173–184.
22. Belo, J. A. *Cerberus-like* is a secreted factor with neuralizing activity expressed in the anterior primitive endoderm of the mouse gastrula. *Mech. Dev.* **68,** 45–57 (1997).
23. Thomas, P., Brickman, J. M., Popperl, H., Krumlauf, R. & Beddington, R. S. Axis duplication and anterior identity in the mouse embryo. *Cold Spring Harb. Symp. Quant. Biol.* **62,** 115–125 (1997).
24. Biben, C. *et al.* Murine cerberus homologue mCer-1: a candidate anterior patterning molecule. *Dev. Biol.* **194,** 135–151 (1998).
25. Topol, L. Z. *et al.* Identification of *drm*, a novel gene whose expression is suppressed in transformed cells and which can inhibit growth of normal but not transformed cells in culture. *Mol. Cell. Biol.* **17,** 4801–4810 (1997).
26. Pearce, J. J., Penny, G. & Rossant, J. A mouse Cerberus/Dan-related gene family. *Dev. Biol.* **209,** 98–110 (1999).
27. Yokouchi, Y., Vogan, K. J., Pearse II, R. V. & Tabin, C. J. Antagonistic signaling by Caronte, a novel Cerberus-related gene, mediates the establishment of broad domains of left-right asymmetric gene expression. *Cell* (in the press).
28. Zhu, L. *et al.* Cerberus regulates left/right asymmetry of the embryonic head and heart. *Curr. Biol.* **9,** 931–938 (1999).
29. Thisse, C. & Thisse, B. Antivin, a novel and divergent member of the TGF_B superfamily, negatively regulates mesoderm induction. *Development* **126,** 229–240 (1999).
30. Meno, C. *et al.* Two closely-related left-right asymmetrically expressed genes, *lefty-1* and *lefty-2*: their distinct expression domains, chromosomal linkage and direct neuralizing activity in *Xenopus* embryos. *Genes Cells* **2,** 513–524 (1997).
31. Oulad-Abdelghani, M. *et al.* Stra3/lefty, a retinoic acid-inducible novel member of the transforming growth factor-β superfamily. *Int. J. Dev. Biol.* **42,** 22–32 (1998).
32. Schneider, A. *et al.* the homeobox gene NKX3.2 is a target of left–right signalling and is expressed on opposite sides in chick and mouse embryos. *Curr. Biol.* **9,** 911–914 (1999).
33. Piccolo, S. *et al.* The head inducer Cerberus is a multifunctional antagonist of Nodal, BMP and Wnt signals. *Nature* **397,** 707–710 (1999).
34. Watanabe, Y. & Le Douarin, N. M. A role for BMP-4 in the development of subcutaneous cartilage. *Mech. Dev.* **57,** 69–78 (1996).
35. Schultheiss, T. M., Burch, J. B. & Lassar, A. B. A role for bone morphogenetic proteins in the induction of cardiac myogenesis. *Genes Dev.* **11,** 451–462 (1997).
36. Streit, A. *et al.* Chordin regulates primitive streak development and the stability of induced neural cells, but is not sufficient for neural induction in the chick embryo. *Development* **125,** 507–519 (1998).
37. Zimmerman, L. B., De Jesus-Escobar, J. M. & Harland, R. M. The Spemann organizer signal noggin binds and inactivates bone morphogenetic protein 4. *Cell* **86,** 599–606 (1996).
38. Capdevila, J. & Johnson, R. L. Endogenous and ectopic expression of noggin suggests a conserved mechanism for regulation of BMP function during limb and somite patterning. *Dev. Biol.* **197,** 205–217 (1998).
39. Pizette, S. & Niswander, L. BMPs negatively regulate structure and function of the limb apical ectodermal ridge. *Development* **126,** 883–894 (1999).
40. Thompson, J. D., Gibson, T. J., Plewniak, F., Jeanmougin, F. & Higgins, D. G. The CLUSTAL_X windows interface: flexible strategies for multiple sequence alignment aided by quality analysis tools. *Nucleic Acids Res.* **25,** 4876–4882 (1997).
41. Mohammadi, M. *et al.* Structures of the tyrosine kinase domain of fibroblast growth factor receptor in complex with inhibitors. *Science* **276,** 955–960 (1997).
42. Izpisua-Belmonte, J. C., De Robertis, E. M., Storey, K. G. & Stern, C. D. The homeobox gene goosecoid and the origin of organizer cells in the early chick blastoderm. *Cell* **74,** 645–659 (1993).
43. Tribioli, C., Frasch, M. & Lufkin, T. *Bapx1:* an evolutionary conserved homologue of the *Drosophila bagpipe* homeobox gene is expressed in splanchnic mesoderm and the embryonic skeleton. *Mech. Dev.* **65,** 145–162 (1997).
44. Olson, E. N. & Srivastava, D. Molecular pathways controlling heart development. *Science* **272,** 671–676 (1996).
45. Harvey, R. P. NK-2 homeobox genes and heart development. *Dev. Biol.* **178,** 203–216 (1996).
46. Meyers, E. N. & Martin, G. R. Differences in left-right axis pathways in mouse and chick: functions of FGF8 and SHH. *Science* **285,** 403–406 (1999).
47. Izraeli, S. *et al.* The SIL gene is required for mouse embryonic axial development and left-right specification. *Nature* **399,** 691–694 (1999).
48. Tsukui, T. *et al.* Multiple left-right asymmetry defects in $Shh^{-/-}$ mutant mice unveil a convergence of the Shh and Retinoic Acid pathways in the control of *Lefty-1*. *Proc. Natl Acad. Sci. USA* (in the press).
49. New, D. A. T. A new technique for the cultivation of the chick embryo in vitro. *J. Embryol. Exp. Morphol.* **3,** 326–331 (1955).
50. Merino, *et al.* Expression and function of Gdf-5 during digit skeletogenesis in the embryonic chick leg bud. *Dev. Biol.* **206,** 33–45 (1999).

Supplementary Information is available at *Nature*'s World-Wide Web site (http://www.nature.com) or as paper copy from the London editorial office of *Nature*.

Acknowledgements

We thank J. Magallón for technical help; T. Brand, R. Evans, H. Hamada, C. Kintner, G. Rosenfeld, C. Stern, C. Tabin and members of P. E. Wright's group for discussions and for sharing unpublished observations; W. Vale and S. Choe for reagents; J. P. Fandl (for providing human Cerberus) and X. Wang (for technical help), both at Regeneron; J. Hurlé for scanning images; C. Parada for suggesting the name Caronte; and L. Hooks for help in preparing the manuscript. J.C. was supported by a Hoffmann Foundation Fellowship; J.P. was supported by a long-term EMBO Fellowship. This work was supported by grants from the G. Harold and Leila Y. Mathers Charitable Foundation and the NIH to J.C.I.B., who is a Pew Scholar.

Correspondence and requests for materials should be addressed to J.C.I.B. (e-mail: belmonte@salk.edu).